Self-consistent system of equations for a kinetic description of the low-pressure discharges accounting for the nonlocal and collisionless electron dynamics

Igor D. Kaganovich
Plasma Physics Laboratory, Princeton University, Princeton, New Jersey 08543, USA

Oleg Polomarov
Department of Physics and Astronomy, University of Toledo, Toledo, Ohio 43606-3390, USA

(Received 1 November 2002; revised manuscript received 9 May 2003; published 22 August 2003)

In low-pressure discharges, where the electron mean free path is larger or comparable with the discharge length, the electron dynamics is essentially nonlocal. Moreover, the electron energy distribution function (EEDF) deviates considerably from a Maxwellian. Therefore, an accurate kinetic description of the low-pressure discharges requires knowledge of the nonlocal conductivity operator and calculation of the non-Maxwellian EEDF. The previous treatments made use of simplifying assumptions: a uniform density profile and a Maxwellian EEDF. In the present study, a self-consistent system of equations for the kinetic description of nonlocal, nonuniform, nearly collisionless plasmas of low-pressure discharges is derived. It consists of the nonlocal conductivity operator and the averaged kinetic equation for calculation of the non-Maxwellian EEDF. The importance of accounting for the nonuniform plasma density profile on both the current density profile and the EEDF is demonstrated.

DOI: 10.1103/PhysRevE.68.026411 PACS number(s): 52.80.Pi

I. INTRODUCTION

Low-pressure radio-frequency discharges are extensively utilized for plasma processing and lighting [1]. Simulation of discharge properties is a common tool for optimization of the plasma density profiles and ion and electron fluxes. Recent plasma technology tends to decrease the gas pressures down to the millitorr range. For these low pressures it is easier to maintain uniform plasmas with well controlled parameters. Due to the large value of the electron mean free path λ the electron current is determined not by the local rf electric field (Ohm's law), but rather is a function of the whole profile of the rf electric field on distances of the order of λ (anomalous skin effect). Therefore, a rather complicated nonlocal conductivity operator has to be determined for the calculation of the rf electric field penetration into the plasma. Moreover, the electron energy distribution function (EEDF) is typically non-Maxwellian in these discharges [2]. Hence, for accurate calculation of the discharge characteristics at low pressures, the EEDF needs to be computed self-consistently. Self-consistency is an important and difficult issue for the kinetic simulations of a plasma. The EEDF, nonlocal conductivity, and plasma density profiles are all nonlinear and nonlocally coupled. That is why, the self-consistency aspect of the model is the main concern of this study. The so-called ''nonlocal'' approach relies on the direct semianalytic solution of the Boltzmann equation in the limiting regime where the electron energy relaxation length is much larger than the discharge gap, but the electron mean free path is small compared with the discharge dimension [3,4]. Under these conditions the EVDF is almost isotropic and can be well approximated as a sum of the main isotropic part of the EVDF, f_0, and small anisotropic part of the EVDF, f_1. Importantly, the main part of the EVDF is a function of the total energy only [$f_0(\varepsilon)$, where $\varepsilon = mv^2/2 - e\phi(\mathbf{r})$, $\phi(\mathbf{r})$ is the electrostatic potential], instead of being a function of velocities and spatial coordinates as in a general case $f_0(\mathbf{r},\mathbf{v})$. *This assumption allows significant simplifications of the Boltzmann equation, which effectively reduces from a six-dimensional* (*three dimensional in coordinate and three dimensional in velocity space*) *problem in phase space to a one-dimensional (1D) problem for* $f_0(\varepsilon)$ *as a function of only* ε. The final 1D equation for the electron energy distribution function is the temporal-spatial averaged Boltzmann equation over the phase space available for the electron with a given total energy ε. The nonlocal approach is the case opposite to the local description of plasma, where $f_0(\mathbf{r},\mathbf{v})$ can be assumed as a function of only kinetic energy and the local rf electric field $f_0(mv^2/2,\mathbf{E}(\mathbf{r}))$, and gradients of the local rf electric field and influence of the ambipolar electric field are neglected. The nonlocal approach has been successfully applied to the self-consistent kinetic modeling of various low-pressure discharges, where the electron mean free path is small: the capacitively coupled plasmas [5,6], the inductively coupled plasmas [7–10], the dc discharges [11,12], the afterglow [13], and the surface-wave discharges [14]. The additional references can be found in reviews [15–17].

If gas pressure is lowered even further (less than 10 mTorr), the electron mean free path becomes comparable or even larger than the discharge dimension, and numerous collisionless phenomena dominate the discharge characteristics [18]. Therefore, wide utilization of low-pressure discharges calls for ''upgrading'' of nonlocal approach by taking into account collisionless phenomena. In the present paper the nonlocal approach is generalized for the low-pressure discharges to incorporate the collisionless heating and transit-time (electron temporal and spatial inertia) effects on plasma conductivity in the discharge description. The main goal of the paper is to derive a general set of equations (formulary) for the nonlocal approach with a rigorous, self-consistent treatment of collisionless phenomena in inhomogeneous-

 ©2003 The American Physical Society

plasmas. Similar approaches have been developed for calculation of the rf heating in tokamaks [23] and for an analysis of kinetic instabilities in intense beams [24].

The derivations are lengthy. Therefore, to be specific, the present analysis considers only an inductively coupled plasma. But the approach has been designed in the most generalized way, so that derivations can be readily performed for other discharges. For example, in Ref. [19] the capacitive discharge; in Ref. [20] the electron-cyclotron-resonance discharge and in Ref. [21] the surface-wave discharge were considered with a self-consistent account for collisionless heating.

Most of the previously reported theoretical studies assume a uniform plasma, in a semi-infinite [22] or a slab geometry [25]. In this case the analytical treatment considerably simplifies, because electron trajectories are straight. In the semi-infinite geometry, electrons traverse the region of the rf electric field (skin layer) and are reflected back into the plasma at the discharge walls. An acquired velocity kick then dissipates in the plasma on distances of the order of the electron mean free path and subsequent kicks can be assumed independent. If the plasma dimension is small or comparable with λ, the subsequent kicks are correlated. The resonance between the wave frequency and the bounce frequency of the electron motion between the walls may result in modification of the nonlocal conductivity [26,27] and may yield an enhanced electron heating [28–30]. The anomalous skin effect has been studied experimentally in cylindrical [26] and planar discharges [31]. Additional references can be found in the reviews of classical and recent works on the anomalous skin effect in gas discharge plasmas [32,33]. The theoretical studies in cylindrical geometry are much more cumbersome, and have been done for uniform plasma in Refs. [34–36] and for a parabolic potential well in Ref. [37]. Qualitative results in the cylindrical geometry are similar to the results in the plane geometry, therefore, in the present study only the one-dimensional slab geometry is considered.

For the case of a bounded uniform plasma, the electrostatic potential well is flat in the plasma and infinite at the wall (to simulate the existence of sheaths). In this square potential well, electrons are reflected back into the plasma only at the discharge walls. In a realistic nonuniform plasma, however, the position of the turning points will depend on the electron's total (kinetic plus potential) energy and the actual shape of the potential well, i.e., low total energy electrons bounce back at locations within the plasma and may not reach regions of high electric field at all. As a result the current density profiles in a nonuniform plasma may considerably differ from the profiles in a uniform plasma. The theory of the anomalous skin effect for an arbitrary profile of the electrostatic potential and a Maxwellian EEDF was developed by Meierovich *et al.* in Refs. [38–40] for the slab geometry. Although some rigorous analytical results of nonuniform plasmas have been reported, the detailed self-consistent, nonlocal simulations related to such plasmas and a comparison with experimental data are lacking. Self-consistent, nonlocal simulations based on the developed, in this paper, approach were completed recently and presented in our separate publications [41,42] and will be additionally reported elsewhere. The alternative approaches to the nonlocal approach are based on particle-in-cell simulations, and only recently were capable of the detailed self-consistent, nonlocal kinetic simulations of low-pressure discharges [43].

The kinetic description of the anomalous skin effect is based on a well known mechanism of collisionless power dissipation—the Landau damping [44]. In the infinite plasma, the resonance particles moving with a velocity $\mathbf{v}$ close to the wave phase velocity, so that $\omega = \mathbf{v}\cdot\mathbf{k}$, intensively interact with wave fields. Therefore, the collisionless electron heating (and the real part of the surface impedance) depends on the magnitude of a Fourier harmonic of the electric field $[E(k)]$ and the number of the resonant particles $[f(v_x=\omega/k),\mathbf{x}\|\mathbf{k}]$. That is why, the momentum acquired in the skin layer of width δ is maximal if the projection of velocity perpendicular to the plasma boundary (x- axis direction) is of the order of $\omega\delta$. If the interaction with the skin layer is repeated in a resonant manner the momentum changes mount up. Therefore, the main contribution to the electron heating and the resistive part of the surface impedance comes from these resonant electrons. The first unambiguous measurements of a bounce-resonance effect were performed in a non-neutral plasma. In Ref. [45] it was shown that the heating rate increases by a factor of 10^4 as the oscillation frequency of the externally applied rf field is increased by a factor of 10 near the thermal electron bounce frequency. In a bounded plasma, the resonance condition requires the bounce period T_b to be equal to one or several rf electric field periods: $T_b = 2\pi n/\omega$, where n is an integer number. The maximum interaction occurs for $n=1$ (see below). For a slab of width L, $T_b = 2L/v_x$. The maximum electron heating occurs if both aforementioned conditions are satisfied simultaneously, which gives $\omega\delta = v_x$ and $2L/v_x = 2\pi/\omega$ or $L=\delta\pi$ [27]. *Hence, the optimum conditions for the power transfer to the plasma corresponds to the plasma of size comparable with three times the skin depth.* Because the bounce frequency depends on the electrostatic potential, accounting for the plasma nonuniformity is important for a correct calculation of the efficient power coupling.

As discussed before, the collisionless heating is determined by the number of resonant particles, and, hence, is dependent on the EEDF. The EEDF, in its turn, is controlled by the collisionless heating. The only particles, which are in resonance with a wave, are heated by the collisionless heating. It means that in the regime of the collisionless dissipation, the form of the electron energy distribution function is sensitive to the wave spectrum. Therefore, the plateau in the EEDF can be formed in the regions of intensive collisionless heating, if the wave phase velocities are confined in some interval [46]. The evidences of a plateau formation for the capacitive discharge plasma were obtained in Ref. [30]. The cold electrons, which are trapped in the discharge center, do not reach periphery plasma regions where an intensive rf electric field is located and, as a result, these electrons are not heated by the rf electric field. The coupling between the EEDF shape and collisionless heating may result in nonlinear phenomena: an explosive generation of the cold electrons [47]. The experimental evidences of the influence of collisionless phenomena on the EEDF shape were obtained in Refs. [31,48–51].

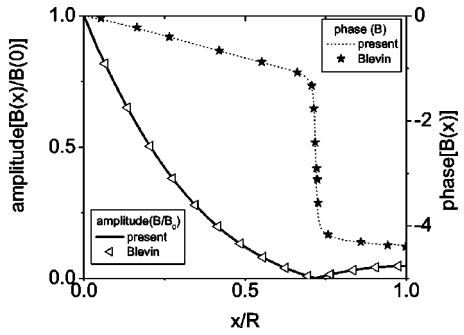

FIG. 1. The normalized magnetic field amplitude and its phase for the case of cylindrical-like geometry (slab geometry and two antisymmetric currents at $x=0$ and $x=L$) as functions of the normalized coordinate x/R, where $R=L/2$. Lines denote the results of the system of equations (25), (27), and (29) and symbols show the results from Ref. [25] for $\omega/\Omega_{bT}=1.5$, $\nu/\Omega_{bT}=0.3$, and $R\omega_p/c=4.5$. The electron temperature is $T_e=2.5$ eV and the uniform spatial electron density is $n_0=10^{12}$ cm^{-3}.

In the linear approximation the collisionless dissipation does not depend explicitly on the collision frequency. However, as shown in Ref. [52], if the electron elastic collision frequency is too small, heating can actually decrease due to nonlinear effects akin of the nonlinear Landau damping. At low frequencies $\omega \ll V_T/\delta$ the nonlinear Lorentz force $eV_{rf}B_{rf}/c$, where V_{rf} is the electron oscillatory velocity, V_T is the thermal velocity ($V_T \equiv \sqrt{2T/m}$), and B_{rf} is the rf magnetic field, has to be taken into account [49,53].

The present paper presents a self-consistent system of equations describing the nonlocal electron kinetics in a 1D slab (bounded) nonuniform plasma. The system consists of a nonlocal conductivity operator and an average over fast electron motion kinetic equation for the EEDF. Transit-time (nonlocal) effects on the current density profile and the collisionless heating are of particular interest. Rigorous derivations for the nonlocal conductivity operator have been performed. The analytic results of Ref. [38] for the Maxwellian EEDF were generalized for the non-Maxwellian EEDF. The spectral method was developed to find the rf electric field profile. A quasilinear approach was used for calculating the collisionless heating. The quasilinear theory developed in Ref. [29] was generalized for an arbitrary value of the collision frequency. As a result, the simulations can be done in a wide range of the background gas pressures ranging from the collisional case ($\lambda \ll \delta$) to the fully collisionless case ($\lambda > L$). Self-consistency of the nonlocal conductivity operator and the energy diffusion coefficient have been verified: both yield the same expression for the power deposition. The robust time-averaging procedure was designed for the kinetic equation in the most general way. As a result, the procedure can be readily repeated for other discharges, see, for example, Refs. [19,20]. Note that the previous papers [41,42] presented self-consistent, nonlocal simulations based on the developed, in this paper, approach. These papers present a comprehensive numerical study and demonstrate a realistic example of the developed approach. Moreover, we have added three numerical examples shown in Figs. 1–3, which demonstrate the developed spectral method for solving the

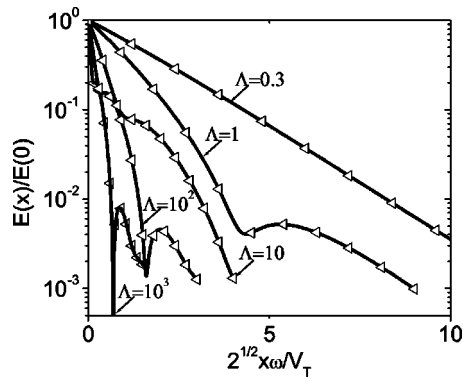

FIG. 2. The normalized electric field amplitude for semi-infinite uniform plasma as a function of normalized depth $|i\omega+\nu|x/v_T$ for $\omega=\nu$ and different $\Lambda=v_T^2\omega_p^2\omega/(c^2|i\omega+\nu|^3)$. Lines denote the results of the system of equations (25), (27), and (29) and symbols show the results from Ref. [22].

Maxwell equation for the rf electric field, not presented in Refs. [41,42]. In Ref. [30] the present approach was applied for capacitive discharge, assuming uniform plasma density in the plasma bulk and taking into account only heating by the oscillating sheaths (neglecting the rf electric field in the plasma bulk). As it was shown in Ref. [19] accounting for the rf electric field in the plasma bulk may lead to significant reduction of the collisionless heating. Therefore, these findings call for different self-consistent calculations of capacitively coupled plasma.

II. CALCULATION OF THE ANISOTROPIC PART OF THE ELECTRON VELOCITY DISTRIBUTION FUNCTION, f_1

In low-pressure discharges, where the energy relaxation length is large compared with the plasma width, the main part of the EVDF is a function of the total energy only [15–17]. Therefore, we look for $f=f_0+f_1$, where $f_0(\varepsilon)$ is a function of the total energy ε, $\varepsilon=w+\varphi(x)$, where w

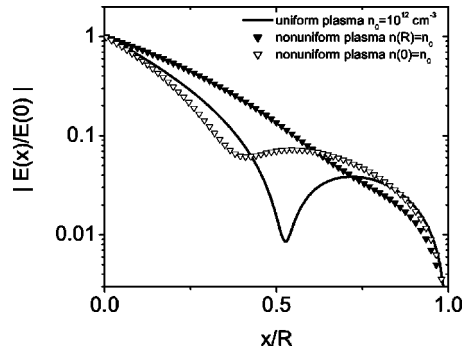

FIG. 3. The profile of the normalized amplitude of the rf electric field calculated for a bounded plasma in a slab geometry with and without the ambipolar potential $\phi=-4(x/R-1)^2$ (in volts) for the same parameters as in Fig. 1 for the following two cases: (1) the electron density at the electrode, $n(0)$, is equal to the electron density of the uniform plasma, n_0, i.e., $n(0)=n_0$ and (2) the electron density in the center, $n(R)$, is equal to n_0, i.e., $n(R)=n_0$, respectively.

$=m(v_x^2+v_y^2+v_z^2)/2$ is the kinetic energy, $\varphi=-e\phi$ is the electron electrostatic potential energy, and ϕ is the electrostatic potential. f_1 does not contribute to the electron density (the integral f_1 over the velocity space is equal to zero $\int f_1 \mathbf{d}^3\mathbf{v}=0$), but f_1 contributes to the electron current (the integral f_0 over the velocity space weighted with the electron velocity is equal to zero $\int \mathbf{v} f_0 \mathbf{d}^3\mathbf{v}=0$). Typically, the mean electron flow velocity ($V^{rf}=\int \mathbf{v} f_1 d^3v/\int f_0 \mathbf{d}^3\mathbf{v}$) is small compared with the thermal velocity V_T. Therefore, the isotropic part of the EVDF is larger than the anisotropic part $f_1 \sim (V^{rf}/V_T) f_0 \ll f_0$ [15–17].

The Boltzmann equation for electron velocity distribution function reads

$$\frac{\partial f_1}{\partial t}+v_x\frac{\partial f_1}{\partial x}-\frac{eE_{sc}(x)}{m}\frac{\partial f_1}{\partial v_x}-\frac{eE_y(x,t)}{m}\frac{\partial (f_0+f_1)}{\partial v_y} = C(f_1+f_0), \tag{1}$$

where $E_{sc}(x)$ is the space-charge stationary electric field, $E_y(x,t)$ is the rf nonstationary electric field, and $C(f)$ is the collision integral. In Eq. (1), we used the fact that

$$v_x\frac{\partial f_0(\varepsilon)}{\partial x}-\frac{eE_{sc}(x)}{m}\frac{\partial f_0(\varepsilon)}{\partial v_x}=v_x\frac{\partial f_0(\varepsilon)}{\partial x}\Big|_{\varepsilon_x}=0, \tag{2}$$

because ε_x is constant along a trajectory. After applying the standard quasilinear theory, Eq. (1) splits into two equations [29]: a linear equation for f_1,

$$\frac{\partial f_1}{\partial t}+v_x\frac{\partial f_1}{\partial x}-\frac{eE_{sc}(x)}{m}\frac{\partial f_1}{\partial v_x}-\frac{eE_y(x,t)}{m}\frac{\partial f_0}{\partial v_y}=C(f_1), \tag{3}$$

and a quasilinear equation for f_0,

$$-\overline{\frac{eE_y(x,t)}{m}\frac{df_1}{dv_y}}=\overline{C(f_0)}, \tag{4}$$

where the overbar denotes space-time averaging over the phase space available for the electron with the total energy ε [54–56].

The rf electric field $E_y(x,t)=E_{y0}(x)\exp(-i\omega t)$ and the anisotropic part of the EVDF $f_1=f_{10}\exp(-i\omega t)$ are harmonic functions, where ω is the discharge frequency. In what follows the subscript 0 is omitted. Equation (3) becomes

$$-i\omega f_1+v_x\frac{\partial f_1}{\partial x}\Big|_{\varepsilon_x}-ev_yE_y(x)\frac{df_0}{d\varepsilon}=-\nu f_1. \tag{5}$$

In the transformation from Eq. (3) to Eq. (5) the Bhatnager-Gross-Krook (BGK) approximation was used $C(f_1)=-\nu f_1$, where ν is the transport collision frequency and we introduced a new variable, namely, the total energy along the x axis, $\varepsilon_x=mv_x^2/2+\varphi(x)$. There have been a number of studies, which explored the effects of the exact collision integral on collisionless phenomena [57,58]. These treatments use expansion in series of spherical functions in velocity spaces. The exact calculations are important only if the collision frequency is a strong function of the polloidal scattering angle. If the differential cross section does not depend on the polloidal scattering angle, the BGK approximation is exactly correct [58]. For partially ionized plasma, the electron-neutral collisions are the most frequent scattering mechanism. In the low-pressure discharges typical electron energies are in the range 1–5 eV [2] and the differential cross section weakly depends on the polloidal scattering angle. As a result, the BGK approximation has a good accuracy [58].

Equation (5) can be solved by a number of different methods. First, let us consider a direct solution. Alternative derivation using Fourier series is performed in Appendix C. After some straightforward algebra described in Appendix A, the symmetric part of the EVDF $f_{1s}\equiv 1/2(f_{1+}+f_{1-})$ is given by

$$f_{1s}(\mathbf{v},\mathbf{x})=-mv_yV_y^{rf}(x,\varepsilon_x)\frac{df_0}{d\varepsilon}, \tag{6}$$

where $V_y^{rf}(x,\varepsilon_x)=1/2(V_{y+}^{rf}+V_{y-}^{rf})$, $V_{y\pm}^{rf}$ are the oscillatory velocities of an electron with a given ε_x, $\pm$ signs denote $v_x>0$ and $v_x<0$, respectively;

$$V_y^{rf}(x,\varepsilon_x,v_\perp)=-\frac{e}{m\sinh\Phi_+}\Bigg[\cosh\Phi\int_x^{x_+}E_y(x')\times\cosh(\Phi_+-\Phi')d\tau'+\cosh(\Phi_+-\Phi)\times\int_{x_-}^{x}E_y(x')\cosh\Phi' d\tau'\Bigg], \tag{7}$$

$$\tau\equiv\int_{x_-}^{x}\frac{dx}{|v_x(x,\varepsilon_x)|}, \tag{8}$$

$$\Phi(x,\varepsilon_x,v_\perp)\equiv\int_{x_-}^{x}(-i\omega+\nu)d\tau, \tag{9}$$

$$\Phi_+(\varepsilon_x,v_\perp)\equiv\Phi(x_+,\varepsilon_x,v_\perp), \tag{10}$$

where $x_-(\varepsilon_x)$ and $x_+(\varepsilon_x)$ are the left and right turning points, respectively, for the electron with energy ε_x [corresponding to zero velocity v_x or $\varepsilon_x=e\varphi(x_-)$], τ is the time of flight from the left turning point $x_-(\varepsilon_x)$ to x, and $v_\perp=\sqrt{v_y^2+v_z^2}$. The functions V_y^{rf} and Φ depend on the electron speed via the collision frequency $\nu(v)$.

In the local limit the electron mean free path is small $\lambda \ll \delta$ and the phase is large $\mathrm{Re}(\Phi)\gg 1$. Therefore, $\cosh\Phi \approx \sinh\Phi \approx 1/2\exp(\Phi)$. The main contribution in both integrals in Eq. (7) are near the point $x'=x$ and, since $d\Phi=(-i\omega+\nu)d\tau$,

$$V_y^{rf}\approx-\frac{e}{m}\frac{E_y(x)}{(-i\omega+\nu)}, \tag{11}$$

as it should be in the local limit.

III. CALCULATION OF NONLOCAL CONDUCTIVITY

Knowing the EVDF f_{1s}, one can calculate the current density

$$j=-\frac{em^{3/2}}{4\pi\sqrt{2}}\int f_{1s}v_y\mathbf{d}^3\mathbf{v}. \tag{12}$$

Substituting f_{1s} from Eq. (6) into Eq. (12) and making the transformation to the spherical coordinates in the velocity space $dv_xdv_ydv_z=v^2dv\sin\vartheta d\vartheta d\psi$ $(\cos\vartheta=v_x/v;\tan\psi=v_y/v_z)$, Eq. (12) becomes

$$j(x)=e\sqrt{2}m^{3/2}\int_0^\infty w\langle v_y^2V_y^{rf}\rangle\frac{df_0(\varepsilon)}{d\varepsilon}dv, \tag{13}$$

where the average over velocity direction factor $\langle v_y^2V_y^{rf}\rangle$ is

$$\langle v_y^2V_y^{rf}\rangle=\frac{v^2}{4\pi}\int_0^\pi\int_0^{2\pi}V_y^{rf}(x,\varepsilon_x,v)[\sin\vartheta]^3[\cos\psi]^2d\psi d\vartheta. \tag{14}$$

Because V_y^{rf}does not depend on ψ, integration over ψ angle can be completed. Changing the integral from ϑ to $v_x=v\cos\vartheta$ gives

$$\langle v_y^2V_y^{rf}\rangle=\frac{1}{4v}\int_{-v}^{v}V_y^{rf}(x,\varepsilon_x,v_\perp)(v^2-v_x^2)dv_x \tag{15}$$

or

$$\langle v_yV_y^{rf}\rangle=\frac{1}{2m\sqrt{w}}\int_{\varphi(x)}^{\varepsilon}V_y^{rf}(x,\varepsilon_x,v_\perp)\frac{\varepsilon-\varepsilon_x}{\sqrt{\varepsilon_x-\varphi(x)}}d\varepsilon_x. \tag{16}$$

Substituting Eq. (16) into Eq. (13) and changing integration from v to ε yields

$$j(x)=\frac{e}{2}\int_{\varphi(x)}^{\infty}\left[\int_{\varphi(x)}^{\varepsilon}\frac{\varepsilon-\varepsilon_x}{\sqrt{\varepsilon_x-\varphi(x)}}V_y^{rf}d\varepsilon_x\right]\frac{df_0(\varepsilon)}{d\varepsilon}d\varepsilon. \tag{17}$$

Further simplifications are possible if the collision frequency ν is small $(\nu\ll\omega)$ or ν does not depend on electron velocity. In this case $V_y^{rf}(x,\varepsilon_x,v_\perp)$ is the only function of (x,ε_x). Integrating Eq. (17) in parts yields

$$j(x)=-\frac{e}{2}\int_{\varphi(x)}^{\infty}\left[\int_{\varphi(x)}^{\varepsilon}\frac{V_y^{rf}(x,\varepsilon_x)}{\sqrt{\varepsilon_x-\varphi(x)}}d\varepsilon_x\right]f_0(\varepsilon)d\varepsilon. \tag{18}$$

If V_y^{rf} is a constant Eq. (18) gives trivial result $j=-enV_y^{rf}$.

Introducing a new function $\Gamma(\varepsilon)$,

$$\Gamma(\varepsilon)\equiv\int_\varepsilon^\infty f_0(\varepsilon)d\varepsilon, \tag{19}$$

and integrating Eq. (18) in parts one more time gives

$$j(x)=-\frac{e}{2}\int_{\varphi(x)}^{\infty}\frac{V_y^{rf}(x,\varepsilon)\Gamma(\varepsilon)}{\sqrt{\varepsilon-\varphi(x)}}d\varepsilon. \tag{20}$$

For the Maxwellian EVDF f_0, Eq. (20) is equivalent to the result of Liberman *et al.* [38].

Substituting Eq. (7) into Eq. (20) yields the nonlocal conductivity operator

$$j_y(x)=\int_0^x G(x,x')E_y(x')dx'+\int_x^L G(x',x)E_y(x')dx', \tag{21}$$

where

$$G(x,x')=\frac{1}{2}\frac{e^2}{\sqrt{2m}}\int_{\max(\varphi,\varphi')}^{\infty}\frac{\cosh\Phi\cosh(\Phi_+-\Phi')}{\sinh\Phi_+}\times\frac{\Gamma(\varepsilon)}{\sqrt{\varepsilon-\varphi(x)}\sqrt{\varepsilon-\varphi(x')}}d\varepsilon. \tag{22}$$

Note that $G(x,x')$ has a logarithmic singularity at $x=x'$ [38], but because calculation of the electron current in Eq. (21) requires additional integration, there is no singularity in the current.

In the limit of large gap, where $\delta<\lambda\ll L$, $\mathrm{Re}(\Phi)\gg1$ and $\cosh\Phi\cosh(\Phi_+-\Phi')/\sinh\Phi_+\to\cosh\Phi\exp(-\Phi')$, and the region of integration in Eq. (21) beyond the skin layer can be omitted. In the local limit, where $\lambda\ll\delta$, Eq. (21) gives the standard local conductivity, see Eq. (11).

IV. CALCULATION OF THE TRANSVERSE rf ELECTRIC FIELD PROFILE

Maxwell's equations can be reduced to a single scalar equation for the transverse electric field [32],

$$\frac{d^2E_y}{dx^2}+\frac{\omega^2}{c^2}E_y=-\frac{4\pi i\omega}{c^2}[j(x)+I\delta(x)-\delta_{anti}I\delta(x-L)], \tag{23}$$

where the electron current j is given by Eq. (21), I is the current in the coil at $x=0$, and $\delta_{anti}=0$, if there is the grounded electrode and no coil with the current located at $x=L$, and $\delta_{anti}=1$, if there is a coil with the current $-I$ at $x=L$. The 1D slab system of two currents flowing in opposite directions describes very well a cylindrical configuration with the radius R, where a coil produces rf currents at both plasma boundaries $x=0$ and $x=2R$, $R=L/2$ [25,26]. Equations (23) and (21) can be solved numerically using a finite difference scheme. There is a major difficulty in such an approach. Straightforward computing of the complex Green's function in Eq. (22) is slow and time consuming [41]. The better approach is to solve the integro-differential equation (23) making use of a spectral method, where the electric field is represented as a sum of harmonic functions.

A. Solving the Maxwell equations for the rf electric field using Fourier series

System that has an antenna at $x=0$ and a grounded electrode at $x=L$ in the uniform plasma was studied theoretically in Ref. [27]. The papers [25,35] considered a cylindrical-like

system in the uniform plasma. Both papers used Fourier series to solve Maxwell's equations. Here, we generalize the procedure for a case of a nonuniform plasma.

Similar to the previous analysis, it is convenient to continue the rf electric field symmetrically $E_y(x)=E_y(-x)$ outside of the slab. Then, the electric field is given by Fourier series [27]

$$E_y(x)=\sum_{s=0}^{\infty}\Xi_s\cos(k_s x), \tag{24}$$

where s is an integer, $k_s=(2s+1)\pi/(2L)$ for the case of the grounded electrode, and $k_s=(2s+1)\pi/L$ for the case of the cylindrical-like system. Substituting Eq. (24) into Eq. (23) and integrating with the weight $2\cos(k_s x)/L$ over the region $[0,L]$ yields

$$\left(-k_s^2+\frac{\omega^2}{c^2}\right)\Xi_s=-\frac{4\pi i\omega}{c^2}\left[j_s+\frac{2I[1+\delta_{anti,k}]}{L}\right], \tag{25}$$

where

$$j_s=\frac{2}{L}\int_0^L j(x)\cos(k_s x)dx. \tag{26}$$

Substituting the equation for the current density from Appendix C, Eq. (C9), gives

$$j_s=\frac{e^2}{m}\frac{1}{(2s+1)\Omega_{bT}}\sum_{l=0}^{\infty}\Xi_l Z_{s,l}^{gen}\left(\frac{\omega+i\nu}{(2s+1)\Omega_{bT}}\right), \tag{27}$$

where $\Omega_{bT}=V_T\pi/L$, and we introduced the generalized plasma dielectric function

$$Z_{s,l}^{gen}(\xi)\equiv\sqrt{\frac{2}{m}}\frac{(2s+1)\pi\Omega_{bT}}{L}\sum_{n=-\infty}^{\infty}\int_0^{\infty}\times\frac{\Gamma(\varepsilon)}{n\Omega_b(\varepsilon)-(2s+1)\Omega_{bT}\xi}\frac{G_{s,n}(\varepsilon)G_{l,n}(\varepsilon)}{\Omega_b(\varepsilon)}d\varepsilon, \tag{28}$$

where the coefficients $G_{l,n}(\varepsilon)$ are the temporal Fourier transform of $\cos(k_l x)$ in the bounce motion of the electron in the potential well $[dx/dt=-eE_{sc}(x)/m]$,

$$G_{l,n}(\varepsilon)=\frac{1}{T}\left[\int_0^T\cos[k_l x(\tau)]\cos\left(\frac{\pi n\tau}{T}\right)d\tau\right]. \tag{29}$$

Finally, the Maxwell equation (25) together with the equations for the electron current (27) and (29) comprise the complete system for determining profiles of the rf electric field.

B. Examples of calculation of rf field profiles for a given EEDF

In the limit of uniform plasma $[E_{sc}(x)=0]$ $\tau=x/v_x$, $T=L/v_x$, and Eq. (29) gives

$$G_{l,n}(\varepsilon)=\frac{1}{L}\left[\int_0^L\cos(k_l x)\cos\left(\frac{n\pi x}{L}\right)dx\right]. \tag{30}$$

For a cylindrical-like system coefficients $G_{l,n}(\varepsilon)$ are particularly simple:

$$G_{l,n}(\varepsilon)=\frac{1}{2}\delta_{(2l+1),|n|}, \tag{31}$$

and the generalized plasma dielectric function for a given Maxwellian EEDF is

$$Z_{s,l}^{gen}(\xi)=\delta_{s,l}Z(\xi), \tag{32}$$

where $Z(\xi)$ is the "standard" plasma dielectric function,

$$Z(\xi)=\pi^{-1/2}\int_{-\infty}^{\infty}dt\frac{\exp(-t^2)}{t-\xi}. \tag{33}$$

System of equations (25), (27), and (29) is identical to the results of Ref. [25] for cylindrical-like configuration uniform plasma with a Maxwellian EEDF. Figure 1 shows the calculated profile of the rf magnetic field and its comparison with the analogous result from Ref. [25] for $\omega/\Omega_{bT}=1.5$, $\nu/\Omega_{bT}=0.3$, and $R\omega_p/c=4.5$, where ω_p is the plasma frequency and $R=L/2$ is the half-width of the slab. The electron temperature is $T_e=2.5$ eV and the uniform spatial electron density is $n_0=10^{12}$ cm^{-3}.

For the case of a sufficiently wide slab ($L\gg V_T/\omega$) the results of the formalism described above coincide with the results from Ref. [22] for a semi-infinite uniform plasma with a Maxwellian EEDF as shown in Fig. 2. The parameter $\Lambda=v_T^2\omega_p^2\omega/(c^2|i\omega+\nu|^3)$ determines the square of the ratio of the effective electron mean free path to the skin depth. The parameter Λ can serve as a measure of "anomality" of the rf field profiles [22]. For example, the rf electric field profiles depart from a simple exponential function for large $\Lambda>0.5$; see Fig. 2.

For a nonuniform plasma taking into account an ambipolar potential makes simulation of the rf field profiles much more cumbersome than for a uniform plasma. Nevertheless, electric field profiles can be effectively computed making use of the fast Fourier transform for numerical computation of $G_{l,n}(\varepsilon)$ coefficients in Eq. (29). The off-diagonal coefficients are generally very small, that is why, utilizing this spectral method, makes computing much faster than the straightforward application of the finite difference method as it was done in Refs. [41,42]. Figure 3 shows the rf electric field profiles calculated for a bounded plasma in a slab geometry with and without the ambipolar potential $\phi=-4(x/R-1)^2$ (in volts) for the same parameters as in Fig. 1 for the following two cases: (1) the electron density at the electrode, $n(0)$, is equal to the electron density of the uniform plasma, n_0, i.e., $n(0)=n_0$ and (2) the electron density in the center, $n(R)$, is equal to n_0, i.e., $n(R)=n_0$, respectively. From Fig. 3 it can be seen that taking into account an ambipolar potential greatly alters the rf electric field profile.

V. AVERAGING OF KINETIC EQUATION FOR THE MAIN PART OF THE EEDF

Kinetic equation for f_0 averaged over the discharge period is

$$v_x \frac{\partial f_0}{\partial x} - \frac{e}{m} E_{sc}(x) \frac{df_0}{dv_x} - \frac{e}{2m} \mathrm{Re}\left[E_y^*(x) \frac{df_1}{dv_y} \right] = C(f_0), \tag{34}$$

$$C(f) = C_{el}^{\mathbf{v}}(f) + C_{el}^{\varepsilon}(f) + C_{ee}(f) + C_{inel}(f), \tag{35}$$

$$C_{el}^{\mathbf{v}}(f) = \int (f' - f) v \, d\sigma, \tag{36}$$

$$C_{el}^{\varepsilon}(f) = \frac{\partial}{v \partial w}(v V_{el} f), \tag{37}$$

$$C_{ee}(f) = \frac{\partial}{v \partial w}\left(v D_{ee} \frac{\partial}{\partial w} f \right) + \frac{\partial}{v \partial w}(v V_{ee} f), \tag{38}$$

$$C_{inel}(f_0) = \sum_k \left[\frac{\sqrt{(w+\varepsilon_k^*)}}{\sqrt{w}} \nu_k^*(w+\varepsilon_k^*) f_0(\varepsilon+\varepsilon_k^*) - \nu_k^* f_0 \right], \tag{39}$$

where $w = mv^2/2$ is the kinetic energy . Here, the elastic collision integral splits into two parts $C_{el}(f) = C_{el}^{\mathbf{v}}(f) + C_{el}^{\varepsilon}(f)$, where $C_{el}^{\mathbf{v}}(f)$ is the part of the elastic scattering collision integral, which takes into account only changes of the electron momentum in the collisions with differential cross section $d\sigma$ and $C_{el}^{\varepsilon}(f)$ accounts for an energy change in the elastic collisions. $C_{ee}(f_0)$ is the electron-electron collision integral and $C_{inel}(f_0)$ is the sum over all inelastic collisions with the electron energy loss ε_k^* and inelastic collision frequency ν_k^* (see Refs. [5,20]) for more details on simulating ionization and wall losses). In Eq. (38), the coefficients D_{ee}, V_{ee}, V_{el} are given by [55,60]

$$V_{el} = \frac{2m}{M} w \nu, \tag{40}$$

$$V_{ee} = \frac{2w\nu_{ee}}{n}\left(\int_0^w dw \sqrt{w} f \right), \tag{41}$$

$$D_{ee} = \frac{4}{3}\frac{w\nu_{ee}}{n}\left(\int_0^w dw w^{3/2} f + w^{3/2} \int_w^\infty dw f \right), \tag{42}$$

$$\nu_{ee} = \frac{4\pi \Lambda_{ee} e^4 n}{m^2 v^3}, \tag{43}$$

where ν_{ee} is the Coulomb collision frequency and Λ_{ee} is the Coulomb logarithm. Note that at large electron energies $\varepsilon \gg T_e$, $V_{ee} \approx 2w\nu_{ee}$, and $D_{ee} \approx 2wT_e\nu_{ee}$, where $T_e = \frac{2}{3}\int_0^w dw w^{3/2} f/n$ and $C_{ee}(f)$ describes relaxation of the EEDF to a Maxwellian.

If the electron energy relaxation length (roughly inelastic electron mean free path $\lambda^* = V_T/\nu_k^*$) is large compared with the gap ($\lambda^* \gg L$), the first two terms on the left hand side of Eq. (34) are dominant and the sum of the first two terms equals to zero (in an asymptotic series with the parameter λ^*/L). Any function of the longitudinal energy $\varepsilon_x \equiv mv_x^2/2 + \varphi(x)$ nullifies the first two terms on the left hand side of Eq. (34). Therefore, f_0 is approximately a function of ε_x only, not a function of both variables x, v_x separately. Similarly, $C_{el}^{\mathbf{v}}(f)$ is the largest term from the remaining terms in the equation. Any isotropic function of the electron speed nullifies $C_{el}^{\mathbf{v}}(f_0) = 0$. To satisfy both conditions: isotropy and to be a function of ε_x, f_0 must be a function of total energy $\varepsilon \equiv mv^2/2 + \varphi(x)$ only [56]. This assumption was verified experimentally in Refs. [16,17,59] and by comparison with particle-in-cell simulations in Ref. [5] for a capacitive coupled plasma, in Refs. [8,36] for a inductive coupled plasma, and in Ref. [20] for an electron cyclotron resonance (ECR) discharge.

To obtain f_0, it is necessary to average Eq. (34) over fast electron bouncing and over all velocity angles. First, let us average over fast electron bouncing. In order to do so, we integrate all terms of Eq. (34) over the full period of electron bouncing,

$$\oint dt L(x, v_x) \equiv \int_{x_-}^{x_+} \frac{dx}{v_x} L(x, v_x > 0) + \int_{x_-}^{x_+} \frac{dx}{|v_x|} L(x, v_x < 0),$$

where $L(x, v_x)$ is a term in Eq. (34). Because the first two terms represent the full time derivative df/dt along the trajectory, they disappear after integration, and Eq. (34) becomes

$$-\oint dt \frac{e}{2m} \mathrm{Re}\left[E_y^*(x) \frac{df_1}{dv_y} \right] = \oint dt C(f_0). \tag{44}$$

Second, we integrate Eq. (44) over all possible perpendicular velocities $dv_y dv_z$ with a given total energy $m(v_y^2 + v_z^2) < 2\varepsilon$ [54,56].

Total averaging is a triple integral

$$\overline{L(x, \mathbf{v})} \equiv \frac{1}{4\pi} \int \int dv_y dv_z \oint dt L(x, \mathbf{v}), \tag{45}$$

where factor $1/4\pi$ is introduced for normalization purposes. Note that integral in Eq. (45) describes averaging over all the phase space available for the electron with the total energy ε, and can be rewritten as

$$\frac{1}{4\pi} \int \int dv_y dv_z \oint dt L(x, \mathbf{v}) = \frac{m}{4\pi} \int dx d^3\mathbf{v} \delta(\varepsilon - w - \varphi(x)) L(x, \mathbf{v}). \tag{46}$$

If $L(x, \mathbf{v})$ depends on the electron velocity only via speed v, which is the case for $C_{el}^{\varepsilon}(f)$, $C_{ee}(f)$, and $C_{inel}(f)$ collision integrals, then integration in Eq. (46) simplifies to become

$$\overline{L(x, \mathbf{v})}(\varepsilon) = \int_{x_-}^{x_+} dx v(x, \varepsilon) L(x, v(x, \varepsilon)), \tag{47}$$

$$v(x,\varepsilon)=\sqrt{2[\varepsilon-\varphi(x)]/m}. \tag{48}$$

Thus, averaging of the collision integral terms, responsible for energy relaxation in Eq. (44), reduces to integrating over the entire available discharge volume weighted with the velocity for an electron with a given total energy ε. This procedure is identical for both collisionless ($\lambda>L$) and collisional ($\lambda\leq L$) cases (compare Eq. (45) with the collisional ($\lambda\leq L$) case [3,4,54]). However, as we shall see next, the electron heating in the rf electric field differs greatly for collisionless and collisional cases.

A. Calculation of the nonlocal energy diffusion coefficient

The term describing electron heating originates from the averaged left hand side of Eq. (44). Making use of the averaging procedure, Eq. (46), the left hand side of Eq. (44) becomes

$$\overline{\frac{eE_y(x,t)}{m}\frac{df_1}{dv_y}}=\frac{e}{8\pi}\int dxd^3\mathbf{v}\delta[\varepsilon-w-\varphi(x)] \times\mathrm{Re}\left[E_y^*(x)\frac{df_1}{dv_y}\right]. \tag{49}$$

Using chain rule for integration in dv_y and the fact that $d\delta(\varepsilon-w-\varphi)/dv_y=mv_y d\delta(\varepsilon-w-\varphi)/d\varepsilon$, Eq. (49) becomes

$$\overline{\frac{eE_y(x,t)}{m}\frac{df_1}{dv_y}}=\frac{em}{8\pi}\frac{d}{d\varepsilon}\mathrm{Re}\int dxd^3\mathbf{v}\delta[\varepsilon-w-\varphi(x)] \times v_yE_y^*(x)f_1. \tag{50}$$

Substituting f_1 from Eq. (6) and integrating in the velocities v_y and v_z yields

$$\overline{\frac{eE_y(x,t)}{m}\frac{df_1}{dv_y}}=\frac{d}{d\varepsilon}D_\varepsilon\frac{df_0}{d\varepsilon}, \tag{51}$$

where we introduced the energy diffusion coefficient D_ε,

$$D_\varepsilon=-\frac{e}{4m}\mathrm{Re}\int_0^\varepsilon d\varepsilon_x(\varepsilon-\varepsilon_x)\int_{x_-(\varepsilon_x)}^{x_+(\varepsilon_x)}\frac{dx}{v_x}E_y^*(x)V_y^{rf}(x,\varepsilon_x). \tag{52}$$

As shown in Appendix B, Eq. (52) is the general expression for the energy diffusion coefficient. In the limiting regime of the small mean free path ($\lambda\ll\delta$), D_ε tends to the known collisional limit [3,4,54]. In the intermediate pressure range ($\delta\ll\lambda\ll L$), Eq. (52) corresponds to the hybrid heating, where the electron motion is collisionless in the skin layer, but the randomization of the velocity kick acquired during a single pass through the skin layer occurs due to collisions in the plasma bulk [28]; and in the collisionless limit, where the mean free path is large ($\lambda>L$), Eq. (52) describes collisionless heating (see Appendixes B and C for details). If the collision frequency does not depend on the kinetic energy the direct substitution of V_y^{rf} from Eq. (7) gives

$$D_\varepsilon(\varepsilon)=\frac{\pi e^2}{4m^2}\sum_{n=-\infty}^{\infty}\int_0^\varepsilon d\varepsilon_x|E_{yn}(\varepsilon_x)|^2\frac{\varepsilon-\varepsilon_x}{\Omega_b(\varepsilon_x)} \times\frac{\nu}{[\Omega_b(\varepsilon_x)n-\omega]^2+\nu^2}, \tag{53}$$

where

$$E_{yn}(\varepsilon_x)=\frac{1}{\pi}\left[\int_0^\pi E_y(\theta)\cos(n\theta)d\theta\right]. \tag{54}$$

Note that expression for $D_\varepsilon(\varepsilon)$ in Eq. (53) accounts for the bounce resonance $\Omega_b(\varepsilon_x)n=\omega$ and the transit-time resonance $\omega=v/\delta$, which corresponds to maxima of $E_{yn}(\varepsilon_x)$.

VI. SELF-CONSISTENT SYSTEM OF EQUATIONS

In summary, the self-consistent system of equations for the kinetic description of low-pressure discharges accounting for nonlocal and collisionless electron dynamics contains the averaged kinetic equation for f_0, the Maxwell equation for the rf electric field, the quasineutrality condition for the electrostatic potential, and the ion density profile given by fluid conservation equations for ion density and ion momentum. These are given as follows.

(1) The averaged kinetic equation for f_0 reads

$$-\frac{d}{d\varepsilon}(D_\varepsilon+\overline{D_{ee}})\frac{df_0}{d\varepsilon}-\frac{d}{d\varepsilon}[\overline{V_{ee}+V_{el}}]f_0 =\sum_k\left[\overline{\nu_k^*(w+\varepsilon_k^*)\frac{\sqrt{(w+\varepsilon_k^*)}}{\sqrt{w}}}f_0(\varepsilon+\varepsilon_k^*)-\overline{\nu_k^*}f_0\right], \tag{55}$$

where the over bar denotes averaging according to Eq. (47), and D_{ee} is given by Eq. (42), V_{ee} by Eq. (41), V_{el} by Eq. (40), and D_ε by Eq. (52) or by Eq. (53).

(2) The rf electric field is determined from the Maxwell equation (23), where the electron current is given by Eq. (21). A robust procedure to solve these equations by the fast Fourier transform method is described by Eqs. (25), (27), and (29).

(3) The electrostatic potential is obtained using the quasineutrality condition

$$n_i(x)=\int_{\varphi(x)}^\infty f_0(\varepsilon)\sqrt{\varepsilon-\varphi(x)}d\varepsilon, \tag{56}$$

where $n_i(x)$ is the ion density profile given by a set of fluid conservation equations for ion density and ion momentum [41]. Euation (56) is solved in the form of a differential equation [5]

$$\frac{d\varphi}{dx}=-T_e^{scr}(x)\frac{d\ln[n_i(x)]}{dx}, \tag{57}$$

where $T_e^{scr}(x)$ is the electron screening temperature,

$$T_e^{scr}(x)=\left[\frac{1}{2n(x)}\int_{\varphi(x)}^{\infty}f_0(\varepsilon)\frac{d\varepsilon}{\sqrt{\varepsilon-\varphi(x)}}\right]^{-1}. \quad (58)$$

(4) The power deposition can be computed as

$$P(x)=\frac{1}{2}\mathrm{Re}[E_y^*(x)j(x)]. \quad (59)$$

Substituting Eq. (17), integrating over the discharge length, and changing the integration order, Eq. (59) becomes

$$P=-\sqrt{2m}\int_0^{\infty}D_{\varepsilon}(\varepsilon)\frac{df_0(\varepsilon)}{d\varepsilon}d\varepsilon. \quad (60)$$

Equation (60) can be used as a consistency check.

ACKNOWLEDGMENTS

This research was supported by the U.S. Department of Energy Office of Fusion Energy Sciences through a University Research Support Program and University of Toledo. The authors gratefully acknowledge helpful discussions with R. Davidson, Badri Ramamurthi, E. Startsev, C. Theodosiou, and L. D. Tsendin.

APPENDIX A: DERIVATION OF f_1

Direct integration of Eq. (5) yields

$$f_{1+}(x,v)=ev_y\frac{df_0}{d\varepsilon}\left[\int_{x_-}^{x}e^{-[\Phi(x)-\Phi(x')]}E'd\tau'+C_1e^{-\Phi(x)}\right], \quad (A1)$$

$$f_{1-}(x,v)=ev_y\frac{df_0}{d\varepsilon}\left[-\int_{x_-}^{x}e^{\Phi(x)-\Phi(x')}E_y'd\tau'+C_2e^{\Phi(x)}\right], \quad (A2)$$

where $\pm$ signs denote $v_x>0$ and $v_x<0$, respectively, and for brevity we introduced $E_y'\equiv E_y(x')$ and $d\tau=dx/|v_x|$, and

$$\Phi(x)\equiv\int_{x_-}^{x}(-i\omega+\nu)d\tau. \quad (A3)$$

The two constants C_1, C_2 are to be determined from the boundary condition at the turning points. The EVDF continues at the turning points

$$f_{1-}(x_-)=f_{1+}(x_-),\quad f_{1-}(x_+)=f_{1+}(x_-). \quad (A4)$$

Substituting the boundary condition at the turning points, Eqs. (A4), into Eqs. (A1) and (A2) yields

$$C_1=C_2\equiv C \quad (A5)$$

and

$$-\int_{x_-}^{x_+}e^{\Phi_+-\Phi'}E_y'd\tau'+Ce^{\Phi_+}=\int_{x_-}^{x_+}e^{-(\Phi_+-\Phi')}E_y'd\tau'+Ce^{-\Phi_+}$$

or

$$C=\frac{1}{\sinh\Phi_+}\int_{x_-}^{x_+}\cosh(\Phi_+-\Phi')E_y'd\tau'. \quad (A6)$$

Here $\Phi\equiv\Phi(x)$, $\Phi'\equiv\Phi(x')$, and $\Phi_+\equiv\Phi(x_+)$. f_1 enters into the current calculation only as a sum $f_{1+}+f_{1-}$. Therefore, we compute $f_{1s}\equiv 1/2(f_{1+}+f_{1-})$ from Eqs. (A1) and (A2),

$$f_{1s}=ev_y\frac{df_0}{d\varepsilon}\left\{C\cosh\Phi-\int_{x_-}^{x}\sinh(\Phi-\Phi')E_y(\theta')d\tau'\right\}, \quad (A7)$$

substituting C from Eq. (A6) gives

$$f_{1s}=-mv_yV_y^{rf}\frac{df_0}{d\varepsilon}, \quad (A8)$$

where

$$V_y^{rf}=-\frac{e}{m}\frac{1}{\sinh\Phi_+}\left[\cosh\Phi\int_{x_-}^{x_+}\cosh(\Phi_+-\Phi')E_y'd\tau'-\sinh\Phi_+\int_{x_-}^{x}\sinh(\Phi-\Phi')E_y'd\tau'\right]. \quad (A9)$$

Splitting the first term into two integrals $\int_{x_-}^{x_+}=\int_{x_-}^{x}+\int_{x}^{x_+}$, and accounting for the fact that

$$\cosh\Phi\cosh(\Phi_+-\Phi')-\sinh\Phi_+\sinh(\Phi-\Phi')=\cosh\Phi'\cosh(\Phi_+-\Phi') \quad (A10)$$

gives

$$V_y^{rf}=-\frac{e}{m}\frac{1}{\sinh\Phi_+}\left[\cosh\Phi\int_{x}^{x_+}E_y'\cosh(\Phi_+-\Phi')d\tau'+\cosh(\Phi_+-\Phi)\int_{x_-}^{x}E_y'\cosh\Phi'd\tau'\right]. \quad (A11)$$

APPENDIX B: DIFFUSION COEFFICIENT IN THE ENERGY SPACE

The equation for the energy diffusion coefficient

$$D_{\varepsilon}=-\frac{e}{4m}\mathrm{Re}\int_0^{\varepsilon}d\varepsilon_x(\varepsilon-\varepsilon_x)\int_{x_-}^{x_+}\frac{dx}{v_x}E_y^*(x)V_y^{rf}(x,\varepsilon_x) \quad (B1)$$

has correct limits in collisional and collisionless cases.

1. Collisional case $\lambda \ll \delta$

In the collisional case, the mean free path is small. Substituting V_y^{rf} from Eq. (11) into Eq. (B1) gives

$$D_\varepsilon = \frac{e^2}{4m^2}\mathrm{Re}\int_0^\varepsilon d\varepsilon_x(\varepsilon-\varepsilon_x)\int_{x_-}^{x_+}\frac{dx}{\sqrt{2(\varepsilon_x-\varphi)/m}} \times \frac{E_y^*(x)E_y(x)}{-i\omega+\nu}. \tag{B2}$$

Changing the order of the integration and accounting for the fact that

$$\frac{1}{m^2}\int_0^\varepsilon d\varepsilon_x\frac{\varepsilon-\varepsilon_x}{\sqrt{2(\varepsilon_x-\varphi)/m}} = \frac{2}{3}v^3,$$

$$D_\varepsilon = \frac{e^2}{6}\mathrm{Re}\int_{x_-}^{x_+}dx|E_y|^2\frac{\nu v^3}{(\omega^2+\nu^2)}, \tag{B3}$$

which corresponds to the collisional case [16,17].

2. Hybrid case $\delta \ll \lambda \ll L$

In the hybrid case, collisions are rare during the electron motion in the skin layer. Therefore, $V_{y\pm}^{rf}$ is simply the velocity ''kick'' due to the rf electric field. Recalling that $V_y^{rf}(x,\varepsilon)=(V_{y+}^{rf}+V_{y-}^{rf})/2$, the last factor in Eq. (B1) can be written as

$$-\frac{1}{2}\frac{e}{m}\int_{x_-}^{x_+}\frac{dx}{v_x}E_y^*(x)V_y^{rf}(x,\varepsilon_x) = \left\langle\frac{1}{2}\oint d\tau\frac{d\Delta V_y(\tau)}{d\tau}\Delta V_y(\tau)\right\rangle = \frac{1}{4}\langle\Delta V_{y\infty}^2\rangle, \tag{B4}$$

where $\oint d\tau$ is an integral along the electron trajectory entering and leaving the skin layer, $\Delta V_{y\infty}$ is the total velocity kick after a single pass through the skin layer, and the angular brackets denote averaging over phases of the rf field. Equation (B1) simplifies to

$$D_\varepsilon = \frac{1}{8}\int_0^\varepsilon d\varepsilon_x(\varepsilon-\varepsilon_x)\langle\Delta V_{y\infty}^2\rangle. \tag{B5}$$

In the limit of a uniform plasma Eq. (B5) was proposed in Refs. [28,36].

3. Collisionless case $\lambda \gg L$

The energy diffusion coefficient, Eq. (B1), is determined by the following integral: $\mathcal{I}=\int_{x_-}^{x_+}E_y^*(x)V_y^{rf}d\tau$. Substitution of V_y^{rf} from Eq. (A11),

$$\mathcal{I} = \frac{1}{\sinh\Phi_+}\int_{x_-}^{x_+}E_y^*(x)d\tau\Bigg[\cosh\Phi\int_x^{x_+}E_y(x') \times\cosh(\Phi_+-\Phi')d\tau' + \cosh(\Phi_+-\Phi) \times\int_{x_-}^{x}E_y(\theta')\cosh\Phi' d\tau'\Bigg].$$

The term in the brackets can be expressed as

$$\cosh\Phi_+\cosh\Phi\int_{x_-}^{x_+}E_y\cosh\Phi' d\tau' + \sinh\Phi_+\Bigg[\cosh\Phi\int_x^{x_+}E_y\sinh\Phi' d\tau' + \sinh\Phi\int_{x_-}^{x}E_y\cosh\Phi' d\tau'\Bigg].$$

Therefore,

$$\mathcal{I} = \frac{\cosh\Phi_+}{\sinh\Phi_+}\int_{x_-}^{x_+}E_y'\cosh\Phi' d\tau'\int_{x_-}^{x_+}E_y^{*'}\cosh\Phi' d\tau' + \mathcal{I}_1,$$

where

$$\mathcal{I}_1 = \int_{x_-}^{x_+}E_y^* d\tau\Bigg[\cosh\Phi\int_x^{x_+}E_y'\sinh\Phi' d\tau' + \sinh\Phi\int_{x_-}^{x}E_y'\cosh\Phi' d\tau'\Bigg].$$

Integrating in parts gives

$$\mathcal{I}_1 = \int_{x_-}^{x_+}\sinh\Phi d\tau\Bigg[\int_{x_-}^{x}[E_y'E_y^*+E_yE_y^*]\cosh\Phi' d\tau'\Bigg].$$

In the collisionless limit, $\sinh\Phi \simeq i\sin\omega\tau+\nu\tau\cos\omega\tau$. Because the energy diffusion coefficient is determined by the real part of the integral and the real part of the phase is small ($\sim\nu$), $\mathcal{I}_1$ can be neglected. Therefore,

$$D_\varepsilon = \frac{e^2}{4m}\mathrm{Re}\int_0^\varepsilon d\varepsilon_x(\varepsilon-\varepsilon_x)\coth\Phi_+\int_{x_-}^{x_+}E_y'\cos\omega\tau' d\tau' \times\int_{x_-}^{x_+}E_y^{*''}\cos\omega\tau'' d\tau'', \tag{B6}$$

where $\sinh\Phi_+\simeq i\sin\omega T+\nu T\cos\omega T$. The main contribution comes from the points where $\omega T=\pi n$ and $\coth\Phi_+ \simeq \pi\Sigma_n\delta(\omega T-\pi n)$:

$$D_\varepsilon(\varepsilon) = \frac{\pi e^2}{4m}\sum_{n=-\infty}^{\infty}\int_0^\varepsilon d\varepsilon_x|Ef|^2(\varepsilon-\varepsilon_x)\delta(\omega T(\varepsilon_x)-\pi n), \tag{B7}$$

$$Ef(\varepsilon_x) = \int_{x_-(\varepsilon_x)}^{x_+(\varepsilon_x)}E_y(x')\cos\omega\tau' d\tau'. \tag{B8}$$

This corresponds to the pervious results of Ref. [29].

APPENDIX C: ALTERNATIVE DERIVATIONS IN FOURIER SPACE

The direct calculations described in the previous sections are rather cumbersome. The alternative derivation can be made easier using Fourier series.

It is convenient to introduce the variable angle of the bounce motion,

$$\theta(x,\varepsilon_x)=\frac{\pi \mathrm{sgn}(v_x)}{T(\varepsilon_x)}\int_{x_-}^{x}\frac{dx}{|v_x(\varepsilon_x)|}, \tag{C1}$$

where T is half of the bounce period of the electron motion in the potential well $\varphi(x)$, which is given by

$$T(\varepsilon_x)=\int_{x_-}^{x_+}\frac{dx}{|v_x(\varepsilon_x)|}. \tag{C2}$$

The bounce frequency for the electron in the potential well is $\Omega_b(\varepsilon_x)=\pi/T(\varepsilon_x)$. Utilizing angle variable, Eq. (5) simplifies to become

$$-i\omega f_1+\Omega_b\frac{\partial f_1}{\partial\theta}|_{\varepsilon_x}-v_y eE_y(\theta)\frac{df_0}{d\varepsilon}=-\nu f_1. \tag{C3}$$

We shall use Fourier series in variable θ:

$$g(x,\varepsilon_x)=\sum_{n=-\infty}^{\infty} g_n \exp(in\theta), \tag{C4}$$

$$g_n=\frac{1}{2\pi}\left[\int_{-\pi}^{\pi} g(\theta,\varepsilon_x)\exp(-in\pi\theta)d\theta\right]. \tag{C5}$$

Note that in the last integral, the region $0<\theta<\pi$ corresponds to $v_x>0$, and the region $-\pi<\theta<0$ corresponds to $v_x<0$. Utilizing Fourier series, Eq. (C5), the Boltzmann equation becomes

$$(in\Omega_b-i\omega+\nu)f_{1n}=eE_{yn}v_y\frac{df_0}{d\varepsilon}, \tag{C6}$$

where

$$E_{yn}(\varepsilon_x)=\frac{1}{\pi}\left[\int_0^{\pi}E_y(\theta)\cos(n\theta)d\theta\right]. \tag{C7}$$

Making use of Fourier series, Eqs. (C4) and (C6), gives

$$f_{1s}(x,\varepsilon_x)=-mv_y V_y^{rf}(x,\varepsilon_x)\frac{df_0}{d\varepsilon},$$

where

$$V_y^{rf}(x,\varepsilon_x)=-\frac{e}{m}\sum_{n=-\infty}^{\infty}\frac{E_{yn}\cos[n\theta(x)]}{in\Omega_b-i\omega+\nu}. \tag{C8}$$

Equation (C8) is the alternative form of Eq. (A11).

Substituting the function $V_y^{rf}(x,\varepsilon_x)$ from Eq. (C8) into Eq. (20) gives the current density

$$j(x)=\frac{e^2}{2m}\sum_{n=-\infty}^{\infty}\int_{\varphi(x)}^{\infty}\frac{\Gamma(\varepsilon)}{\sqrt{\varepsilon-\varphi(x)}}\frac{E_{yn}\cos[n\theta(x)]}{in\Omega_b-i\omega+\nu}d\varepsilon. \tag{C9}$$

The averaged energy coefficient is given by Eq. (B1). Substituting the function $V_y^{rf}(x,\varepsilon_x)$ from Eq. (C8) into Eq. (B1) gives

$$D_\varepsilon=\frac{e^2}{4m^2}\mathrm{Re}\int_0^{\varepsilon}d\varepsilon_x(\varepsilon-\varepsilon_x)\int_{x_-}^{x_+}\frac{dx}{v_x}E_y^*(x)\times\sum_{n=-\infty}^{\infty}\frac{E_{yn}\cos[n\theta(x)]}{in\Omega_b-i\omega+\nu}$$

or

$$D_\varepsilon(\varepsilon)=\frac{\pi e^2}{4m^2}\sum_{n=-\infty}^{\infty}\int_0^{\varepsilon}d\varepsilon_x\frac{|E_{yn}(\varepsilon_x)|^2(\varepsilon-\varepsilon_x)\nu}{\Omega_b(\varepsilon_x)\{[\Omega_b(\varepsilon_x)n-\omega]^2+\nu^2\}}. \tag{C10}$$

Note that Eq. (C10) is valid for any collision frequency and Eq. (B7) is valid only for $\nu\ll\omega$.

[1] M. A. Lieberman and A. J. Lichtenberg, *Principles of Plasma Discharges and Materials Processing* (Wiley, New York, 1994).

[2] V. A. Godyak, R. B. Piejak, and B. M. Alexandrovich, Plasma Sources Sci. Technol. **11**, 525 (2002).

[3] I.B. Bernstein and T. Holstein, Phys. Rev. **94**, 1475 (1954).

[4] L.D. Tsendin, Sov. Phys. JETP **39**, 805 (1974).

[5] S.V. Berezhnoi, I.D. Kaganovich, and L.D. Tsendin, Plasma Sources Sci. Technol. **7**, 268 (1998).

[6] S.V. Berezhnoi, I.D. Kaganovich, M. Mišina, A. Bogaerts, and R. Gijbels, IEEE Trans. Plasma Sci. **27**, 1339 (1999).

[7] V.I. Kolobov and W.N.G. Hitchon, Phys. Rev. E **52**, 972 (1995).

[8] V.I. Kolobov, G.J. Parker, and W.N.G. Hitchon, Phys. Rev. E **53**, 1110 (1996).

[9] U. Kortshagen, I. Pukropski, and L.D. Tsendin, Phys. Rev. E **51**, 6063 (1995).

[10] G. Muemkin, J. Phys. D **32**, 804 (1999).

[11] V.I. Kolobov and L.D. Tsendin, Phys. Rev. E **46**, 7837 (1992).

[12] Yu. Benke *et al.*, Tech. Phys. **39**, 33 (1994).

[13] R.R. Arslanbekov and A.A. Kudryavtsev, Phys. Rev. E **58**, 7785 (1998).

[14] Yu. M. Aliev, H. Schlueter, and A. Shivarova, *Guided-Wave-Produced Plasmas* (Springer, Berlin, 2000), Chap. 6.

[15] L.D. Tsendin, Plasma Sources Sci. Technol. **4**, 200 (1995).

[16] V.I. Kolobov and V.A. Godyak, IEEE Trans. Plasma Sci. **23**, 503 (1995).

[17] U. Kortshagen, C. Busch, and L.D. Tsendin, Plasma Sources

Sci. Technol. **5**, 1 (1996).
[18] M.A. Lieberman and V.A. Godyak, IEEE Trans. Plasma Sci. **26**, 955 (1998).
[19] Igor D. Kaganovich, Phys. Rev. Lett. **89**, 265006 (2002); and a fuller version in http://arxiv.org/PS_cache/physics/pdf/0203/0203042.pdf
[20] I.D. Kaganovich, M. Mišina, R. Gijbels, and S.V. Berezhnoi, Phys. Rev. E **61**, 1875 (2000).
[21] Yu.M. Aliev, U. Kortshagen, A.V. Maximov, H. Schlueter, and A. Shivarova, Phys. Rev. E **51**, 6091 (1995).
[22] E.S. Weibel, Phys. Fluids **10**, 741 (1967).
[23] Dirk Van Eester, J. Plasma Phys. **65**, 407 (2001).
[24] E. Startsev and R. C. Davidson (private communication).
[25] H.A. Blevin, J.A. Reynolds, and P.C. Thonemann, Phys. Fluids **13**, 1259 (1970).
[26] H.A. Blevin, J.A. Reynolds, and P.C. Thonemann, Phys. Fluids **16**, 82 (1973).
[27] K.C. Shaing and A.Y. Aydemir, Phys. Plasmas **4**, 3163 (1997).
[28] I.D. Kaganovich, V.I. Kolobov, and L.D. Tsendin, Appl. Phys. Lett. **69**, 3818 (1996).
[29] Yu.M. Aliev, I.D. Kaganovich, and H. Schluter, Phys. Plasmas **4**, 2413 (1997); and in more detail, Yu. M. Aliev, I. D. Kaganovich, and H. Schluter, in *Collisionless Electron Heating in RF Gas Discharges. I. Quasilinear Theory*, Vol. 367 of *NATO Advanced Studies Institute, Series B: Physics*, edited by U. Korsthagen and L. Tsendin (Plenum Press, New York, 1998).
[30] U. Buddemeier and I. Kaganovich, in *Collisionless Electron Heating in RF Gas Discharges. II. Role of Collisions and Nonlinear Effects*, Vol. 367 of *NATO Advanced Studies Institute, Series B: Physics*, edited by U. Korsthagen and L. Tsendin (Plenum Press, New York, 1998).
[31] V.A. Godyak and R.B. Piejak, J. Appl. Phys. **82**, 5944 (1997).
[32] V.I. Kolobov and D.J. Economou, Plasma Sources Sci. Technol. **6**, 1 (1997).
[33] F.F. Chen, Phys. Plasmas **8**, 3008 (2001).
[34] B.E. Meierovich, Sov. Phys. JETP **10**, 782 (1970).
[35] N.S. Yoon, S.S. Kim, C.S. Chang, and Duk-In Choi, Phys. Rev. E **54**, 757 (1996).
[36] V.I. Kolobov, D.P. Lymberopoulos, and D.J. Economou, Phys. Rev. E **55**, 3408 (1997).
[37] R.G. Storer, Phys. Fluids **16**, 949 (1973).
[38] M.A. Liberman, B.E. Meierovich, and L.P. Pitaevskii, Sov. Phys. JETP **35**, 904 (1972).
[39] S.M. Dikman and B.E. Meierovich, Sov. Phys. JETP **37**, 835 (1973).
[40] A.N. Vasiliev and B.E. Meierovich, Sov. Phys. JETP **40**, 865 (1974).
[41] B. Ramamurthi, D.J. Economou, and I.D. Kaganovich, Plasma Sources Sci. Technol. **12**, 170 (2002); see http://arxiv.org/ftp/physics/papers/0208/0208053.pdf
[42] B. Ramamurthi, D. J. Economou, and I. D. Kaganovich, Plasma Sources Sci. Technol. **12**, 302 (2003); see http://arxiv.org/ftp/physics/papers/0208/0210114.pdf
[43] V. Vasenkov and M.J. Kushner, Phys. Rev. E **66**, 066411 (2002).
[44] L.D. Landau, J. Phys. (Moscow) **10**, 25 (1946).
[45] B.P. Cluggish, J.R. Danielson, and C.F. Driscoll, Phys. Rev. Lett. **81**, 353 (1998).
[46] A. A. Vedenov, in *Theory of a Weakly Turbulent Plasma*, Reviews of Plasma Physics Vol. 3, edited by M. A. Leontovich (Consultants Bureau, New York, 1967).
[47] S.V. Berezhnoi, I.D. Kaganovich, and L.D. Tsendin, Plasma Phys. Rep. **24**, 556 (1998).
[48] V.A. Godyak and V.I. Kolobov, Phys. Rev. Lett. **81**, 369 (1998).
[49] V.A. Godyak, B.M. Alexandrovich, and V.I. Kolobov, Phys. Rev. E **64**, 026406 (2001).
[50] Chin Wook Chung, K.-I. You, S.H. Seo, S.S. Kim, and H.Y. Chang, Phys. Plasmas **8**, 2992 (2001).
[51] Chin Wook Chung, S.S. Kim, S.H. Seo, and H.Y. Chang, J. Appl. Phys. **88**, 1181 (2000).
[52] I.D. Kaganovich, Phys. Rev. Lett. **82**, 327 (1999).
[53] Yu. O. Tyshetskiy, A. I. Smolyakov, and V. A. Godyak, Phys. Rev. Lett. **90**, 255002 (2003).
[54] L.D. Tsendin and Yu.B. Golubovskii, Sov. Phys. Tech. Phys. **22**, 1066 (1977).
[55] I.D. Kaganovich and L.D. Tsendin, IEEE Trans. Plasma Sci. **20**, 66 (1992).
[56] I.D. Kaganovich and L.D. Tsendin, IEEE Trans. Plasma Sci. **20**, 86 (1992).
[57] W.W. Lee, R.H. Hirsch, and J. Devait, Phys. Fluids **14**, 941 (1971).
[58] E. Furkal, A. Smolyakov, and A. Hirose, Phys. Rev. E **58**, 965 (1998).
[59] Chin Wook Chung and Hong-Young Chang, Phys. Plasmas **7**, 3826 (2000).
[60] V.L. Ginzburg and A.V. Gurevich, Sov. Phys. Usp. **3**, 115 (1960).